On The Relations between SINR Diagrams and Voronoi Diagrams

Merav Parter and David Peleg

The Weizmann Institute of Science, Rehovot, Israel.
{merav.parter,david.peleg}@ weizmann.ac.il *

Abstract. In this review, we illustrate the relations between wireless communication and computational geometry. As a concrete example, we consider a fundamental geometric object from each field: SINR diagrams and Voronoi diagrams. We discuss the relations between these representations, which appear in several distinct settings of wireless communication, as well as some algorithmic applications.

1 Introduction

Wireless networks are embedded in our daily lives, with an ever-growing use of cellular, satellite and sensor networks. Subsequently, the capacity of wireless networks, i.e., the maximum *achievable rate* by which stations can communicate reliably, has received an increasing attention in recent years [15, 20, 18, 14, 7, 2, 16]. The great advantage of wireless communication, namely, the broadcast nature of the medium, also creates its biggest obstacle – interference. When a receiver has to decode a message (i.e., a signal) sent from a transmitter, it must cope with all other (legitimate) simultaneous transmissions by neighboring stations.

While the physical properties of channels have been thoroughly studied [13, 22], less is known about the topology and geometry of the wireless network structure and their influence on performance. This review concerns a novel approach recently proposed to describe the behavior of multi-station networks, which is based on building a *reception map* according to the *signal-to-interference & noise ratio (SINR)* model. By now, the SINR model is the most commonly studied abstract physical model for wireless communication networks, widely used by both the Electrical Engineering community and the algorithmic computer science community. This physical model aims at gauging the quality of signal reception at the receivers while faithfully representing phenomena such as attenuation and interference. Specifically, in this model, the signal decays as it travels and a transmission is successful if its strength at the receiver exceeds the accumulated signal strength of interfering transmissions by a sufficient (technology determined) factor.

* Supported in part by the Israel Science Foundation (grant 894/09) and the Israel Ministry of Science and Technology (infrastructures grant).

The SINR model gives rise to a natural geometric object, the *SINR* diagram, which partitions the plane into a reception region $H(s_i)$ per station $s_i \in S$ and the remaining area $H(\emptyset)$ where none of the stations are heard. Each of these $n+1$ regions may possibly be composed of several disconnected regions.

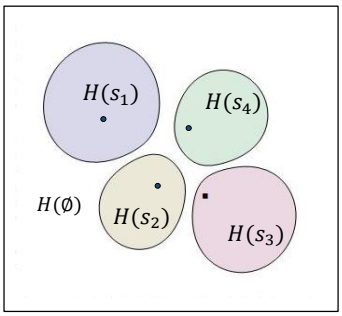

SINR Diagram

SINR diagrams have been recently studied from topological and geometric standpoints [6, 17, 5], and they appear to provide improved understanding on the behavior of wireless networks. Specifically, these diagram have been shown to play a central role in the development of several approximation and online algorithms (e.g., point location tasks, map drawing). Such a role is analogous perhaps to the role played by *Voronoi diagrams* in the study of proximity queries and other algorithms in computational geometry.

The ordinary Voronoi diagram on a given set of points S tessellates the space in such a way that every location is assigned to the closest point in S, thus partitioning the space into *regions* $\textsc{Vor}(s_i)$, each consisting of the set of locations closest to one point in S (referred to as the region's *generator*).

In this review, we focus on the analogy between these two space partitions, the SINR diagrams and the Voronoi diagrams. At first glance, the connection is not immediate. SINR diagrams are based upon the physics of the wireless communication, and geometry is only one aspect of it. In contrast, Voronoi diagrams are mainly based on the geometry of the point arrangement. In addition, whereas Voronoi diagrams are mostly based on the pairwise relations between the generators (i.e., the points of S, referred to as stations in the wireless terminology), in an SINR diagram the reception region of s_i is determined by a complex relation to all other stations and cannot be represented in general as a collection of pairwise relations.

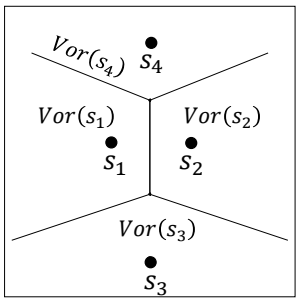

Despite these distinctions, the connections between these diagrams appear to be persistent and re-occur in several *distinct* settings of wireless communications (in fact, in any setting that has been studied so-far). We also exemplify several algorithmic and theoretical applications of these relations.

Let us remark that this review restricts attention to the *static* setting (i.e., where the locations of the network stations are fixed). Turning to the stochastic

setting, the relations between stochastic SINR diagram (formed by modeling the SINR as a marked point process) and classical stochastic geometry models such as PoissonVoronoi tessellations, have been studied extensively, and are out of the scope of this review. See [8] for a detailed analysis, results and applications of this approach.

The structure of this review is as follows. In Sec. 2 we provide a brief overview of SINR diagrams. We then describe the connections between SINR diagrams and Voronoi diagrams in three main settings. Sec. 3 considers the *uniform power* setting, when all stations have the same transmission power. In Sec. 4, we consider the general setting of *non-uniform power* (i.e., when the transmission powers are arbitrary). Finally, in Sec. 5, we describe a setting in which receivers are allowed to employ a decoding technique known as *interference cancellation* to improve their reception quality. In each of these settings, the resulting SINR diagrams turn out to correspond to some variant of Voronoi diagrams, as elaborated on in what follows.

2 Wireless Networks and SINR

We consider a wireless network $\mathcal{A} = \langle d, S, \psi, N, \beta, \alpha \rangle$, where $d \in \mathbb{Z}_{\geq 1}$ is the dimension, $S = \{s_1, s_2, \ldots, s_n\}$ is a set of transmitting *radio stations* embedded in the d-dimensional space, ψ is an assignment of a positive real *transmitting power* ψ_i to each station s_i, $N \geq 0$ is the *background noise*, $\beta \geq 1$ is a constant that serves as the *reception threshold*, and $\alpha > 0$ is the *path-loss parameter*. The *signal to interference & noise ratio (SINR)* of s_i at point p is defined as

$$\mathrm{SINR}_{\mathcal{A}}(s_i, p) \;=\; \frac{\psi_i \cdot \mathrm{dist}(s_i, p)^{-\alpha}}{\sum_{j \neq i} \psi_j \cdot \mathrm{dist}(s_j, p)^{-\alpha} + N} \;. \tag{1}$$

The fundamental rule of the SINR model is that the transmission of station s_i is received correctly at point $p \notin S$ if and only if its SINR at p reaches or exceeds the reception threshold of the network, i.e., $\mathrm{SINR}_{\mathcal{A}}(s_i, p) \geq \beta$. When this happens, we say that s_i is *heard* at p.

We refer to the set of points that hear station s_i as the *reception region* of s_i, defined as

$$H(s_i, \mathcal{A}) \;=\; \{p \in \mathbb{R}^d - S \mid \mathrm{SINR}_{\mathcal{A}}(s_i, p) \geq \beta\} \cup \{s_i\} \;. \tag{2}$$

(Note that $\mathrm{SINR}(s_i, \cdot)$ is undefined at points in S and in particular at s_i itself.) Analogously, the set of points that hear no station $s_i \in S$ (due to the background noise and interference), the *null region*, is defined as

$$H(\emptyset, \mathcal{A}) \;=\; \{p \in \mathbb{R}^d - S \mid \mathrm{SINR}(s_i, p) < \beta, \quad \forall s_i \in S\}.$$

An SINR diagram

$$\mathcal{H}(\mathcal{A}) = \left(\bigcup_{s_i \in S} H(s_i, \mathcal{A}) \right) \cup H(\emptyset, \mathcal{A})$$

is a "reception map" characterizing the reception regions of the stations. When the network $\mathcal{A}$ is clear from the context, we may omit it, and simply write $\mathrm{SINR}(s_i, p), H(s_i)$ and $H(\emptyset)$.

3 Uniform SINR Diagram and Voronoi Diagram

The study of SINR diagram has been initiated by Avin et al. in [6] for the relatively simple case where all stations use the same transmission power, a.k.a, *uniform power* (i.e., $\psi_i = 1$ for every station s_i in Eq. (1)). It has been shown that under this setting, the SINR diagram assumes a rather convenient form. In particular, for SINR threshold $\beta \geq 1$, it holds that every reception region $H(s_i)$ is convex and fat (see Fig. 1(a) for schematic illustration of these notions).

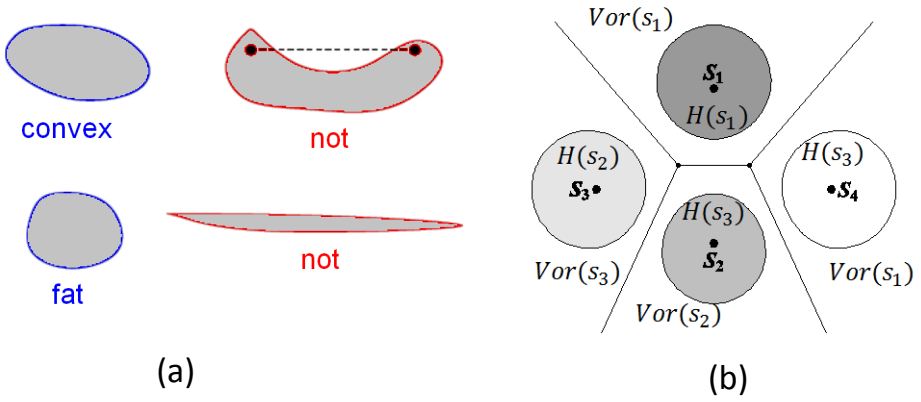

Fig. 1. (a) Uniform SINR regions are "nice": convex and fat. (b) Illustration of the relations between uniform SINR diagram and Voronoi diagram. The reception region $H(s_i)$ is fully contained in the corresponding Voronoi region $\textsc{Vor}(s_i)$.

Let $\textsc{Vor}(s_i)$ be the Voronoi region of station s_i, defined by

$$\textsc{Vor}(s_i) = \{p \in \mathbb{R}^d \mid \mathrm{dist}(s_i, p) \leq \mathrm{dist}(s_j, p),, \text{ for any } j \neq i\} . \qquad (3)$$

Since all transmission powers are the same, for a receiver p that successfully receives the transmission of s_i, it must hold that s_i is the closest station to p among all other network stations, i.e., that $p \in \textsc{Vor}(s_i)$. This condition is not sufficient for successful reception, and hence uniform SINR diagrams can be considered as a *refinement* of Voronoi diagrams. The refinement stems from that fact that the SINR model (even in the uniform case) takes into consideration not only the geometry but also other physical parameters such as attenuation and fading of signals.

The following lemma from [6] formalizes this intuition by claiming that the reception region $\mathcal{H}(s_i, \mathcal{A})$ is strictly contained in the corresponding Voronoi region $\textsc{Vor}(s_i)$.

Lemma 1 (Uniform SINR Diagram and Voronoi Diagram, [6]). *For uniform network $\mathcal{A} = \langle d, S, \overline{1}, N, \beta \geq 1, \alpha \rangle$, it holds that $H(s_i, \mathcal{A}) \subseteq \textsc{Vor}(s_i)$ for every $s_i \in S$.*

See Fig. 1(b). In fact, this analogy between the two diagrams becomes stronger when the path-loss parameter α tends to infinity and there is no ambient noise $N = 0$. The case of noisy SINR diagram with $\alpha \to \infty$ and $N > 0$ is more involved and can be shown to converge to alpha shapes [11].

Note that when $\beta < 1$, the inclusion between the SINR diagram and the Voronoi diagram may no longer hold. That is, it is possible to identify points $p \in \mathbb{R}^d$, for which $\mathrm{SINR}(s_i, p) \geq \beta$ while $p \notin \textsc{Vor}(s_i)$.

Algorithmic application: Point Location. In the *Point Location* task, one is given an n-station wireless network $\mathcal{A}$ and a query point p referred to as a point-location query. The goal is to identify which of the stations is heard at p, if any. As it is assumed that the reception threshold satisfies $\beta \geq 1$, if there is noise $N \geq 0$, then at most one station can be heard at p. The trivial procedure for answering the query is to evaluate the SINR function $\mathrm{SINR}(s_i, p)$ at each of the stations $s_i \in S$, which takes linear time in the number of stations n. To facilitate multiple queries, one may want to build a data structure that can guarantee faster response.

By exploiting the fatness and convexity of the reception regions as well as the relation to Voronoi diagrams, [6] proposed an *approximate* point location scheme that answers point location queries in $O(\log n)$ time. This scheme consists of a preprocessing step in which the Voronoi diagram and "approximated" reception SINR regions $\widetilde{H}(s_i)$ for every $s_i \in S$ are constructed. Answering a point-location query p then involves two main steps. First, the sole candidate station s_p that may be heard at p is identified by finding the Voronoi cell to which p belongs (this can be done in logarithmic time). The second step then uses the approximated region $\widetilde{H}(s_p)$ (constructed in the preprocessing step) to decide whether $\mathrm{SINR}(s_p, p) \geq \beta$. For an efficient batched point location schemes, see the recent [3].

4 Non-uniform SINR Diagram and Weighted Voronoi Diagram

In many actual wireless communication systems, wireless communication devices can modify their transmission power. Moreover, it has been demonstrated convincingly that allowing transmitters to use different power levels increases the efficiency of various communication patterns. It is therefore important to study the topology of SINR diagrams with non-uniform power (i.e., when the transmission powers are arbitrary). This general setting has been considered in [17]. The first observation of [17] is the unfortunate fact that non-uniform diagrams are more complicated than in the uniform case. In particular, the reception regions are no longer convex or even connected. That is, a reception region may consist of several disconnected "reception islands".

For example, the reception region of s_1 in the figure consists of two disconnected components. The loss of the nice properties established for the uniform setting motivated the definitions of alternative notions of weaker convexity. Another important research direction involves bounding the maximum number of connected components, that an n-station wireless network may assume.

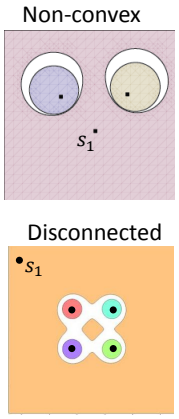

Several important properties of SINR diagrams were established in [17]. One of the key results demonstrates that the reception regions in $\mathbb{R}^{d+1}$ (i.e., drawing the SINR diagram in one dimension higher than that in which the stations are embedded) are *hyperbolically convex*; see Fig. 2. Hence, although the d-dimensional map might be highly fractured, drawing the map in one dimension higher "heals" the regions, which become (hyperbolically) connected.

In the context of Voronoi diagrams, in contrast to the uniform case, the reception regions of a non-uniform SINR diagram are not necessarily contained in the corresponding Voronoi regions. Clearly, the reception region of a very strong station (i.e., with sufficiently large transmission power) may exceed its corresponding Voronoi region. The asymmetry that arises by non-uniform power assignments calls for a *weighted* variant of Voronoi diagram. Specifically, [17] showed that SINR diagrams with *non-uniform* powers are related to *multiplicatively-weighted Voronoi* diagrams (see [4]).

In the (multiplicatively) weighted version of Voronoi diagram [4], every generator (i.e., station) s_i is given a weight w_i that expresses the capability of s_i to influence its neighborhood. Formally, the weighted system $V = \langle S, W \rangle$ consists of $S = \{s_1, ..., s_n\}$, which represents a set of n points or generators in d-dimensional Euclidean space, and $W = \{w_1, ..., w_n\}$, which is an assignment of weights $w_i \in \mathbb{R}_{>0}$ to each point $s_i \in S$. The *weighted voronoi diagram* of

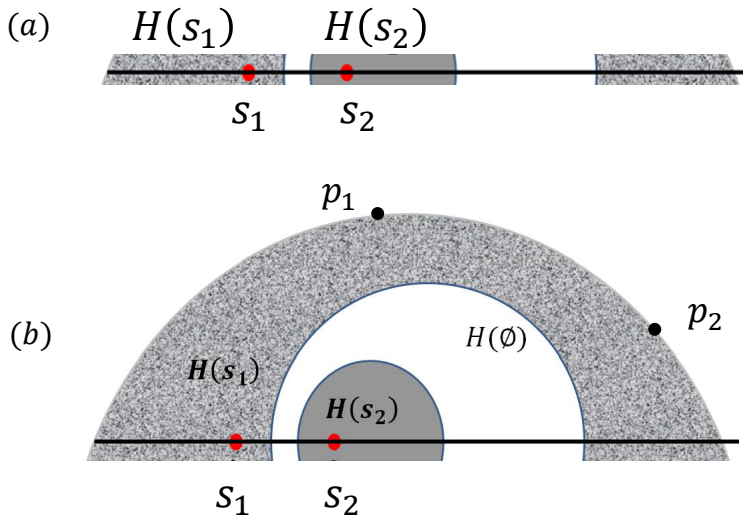

Fig. 2. Reception regions are hyperbolic-convex in $\mathbb{R}^{d+1}$. The given network consists of two stations s_1 and s_2 aligned on a line (i.e., one-dimensional network). (a) The recepetion region $H(s_1)$ of s_1 is not connected in $\mathbb{R}^1$. (b) The reception region of s_1 is connected in $\mathbb{R}^2$. The hyperbolic line connecting two reception points p_1 and p_2 is fully contained in the 2-dimensional reception region $H(s_1)$.

$V = \langle S, W \rangle$ partitions the space into n regions, where

$$\text{WVOR}(s_i) \;=\; \left\{ p \in \mathbb{R}^d \mid \frac{w_i}{\text{dist}(s_i, p)} \;\geq\; \frac{w_j}{\text{dist}(s_j, p)}, \text{ for any } j \neq i \right\} \qquad (4)$$

denotes the region of influence of the generator s_i in S, for every $i \in \{1, \ldots, n\}$. Note that when all the weights are the same, Eq. (4) is equivalent to Eq. (3), i.e., the weighted Voronoi diagram is the same as the ordinary Voronoi diagram. Unlike the ordinary Voronoi diagram, the weighted Voronoi region $\text{WVOR}(s_i)$ is *not* necessarily connected and the diagram may consist of $\Omega(n^2)$ components.

Given a non-uniform wireless network $\mathcal{A}$ with transmission powers $\psi_1, \ldots, \psi_n$, the corresponding weighted Voronoi system is given by setting the weight of each station $s_i \in S$ to

$$w_i = \psi_i^{1/\alpha} \;, \qquad (5)$$

where α is the path-loss parameter of the wireless network. This weight adjustment yields the next lemma, the analogue of Lemma 2 for the non-uniform case.

Lemma 2 (non-uniform SINR Diagram and Weighted Voronoi Diagram, [17]). *Let $\mathcal{A}$ be a non-uniform network. Then $H(s_i, \mathcal{A}) \subseteq \text{WVOR}(s_i)$ for every $s_i \in S$, where the weights of the weighted Voronoi diagram are set according to Eq. (5) (see Fig. 3).*

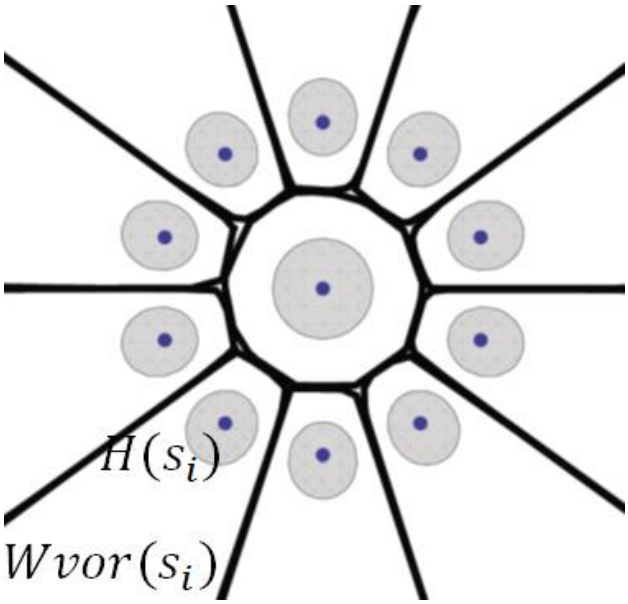

Fig. 3. The reception regions of the non-uniform SINR diagram are strictly contained in the corresponding weighted Voronoi regions upon setting the weights according to Eq. (5).

Note that the weight assignment of Eq. (5) tends to 1 as the path-loss parameter α tends to infinity. Hence, the non-uniform SINR diagram converges to the ordinary (non-weighted) Voronoi diaram as α tends to infinity. (Intuitively, as α gets larger, the distances dominate the effect of the transmission powers.)

Similarly to the uniform case, the relation to weighted Voronoi diagram is found to be useful for solving point location queries efficiently. We conclude this

section by providing an example in which weighted Voronoi diagrams are *not* helpful, due to some fundamental differences between the two models.

Example illustrating the gap between SINR and Voronoi diagram. Establishing a tight universal bound for the number of connected components in the SINR diagram of an n-station network is one of the main open challenges in the study of non-uniform SINR networks. A seemingly promising approach to studying this question is considering it on the corresponding weighted Voronoi diagrams. Since any non-uniform SINR region is fully contained in a corresponding weighted Voronoi region, it seems plausible that the number of weighted Voronoi cells (bounded by $O(n^2)$ [4]) might upper bound the number of connected components in the corresponding SINR diagram. Unfortunately, this does not hold in general, since it might be the case that a single weighted Voronoi component contains a disconnected SINR region. This scenario is illustrated in the figure below and emphasizes a fundamental gap between the SINR and Voronoi diagrams.

The first figure depicts a non-uniform network $\mathcal{A}$ with stations $S = \{s_1, \ldots, s_n\}$ and transmission powers $\psi = \{\psi_1, \ldots, \psi_n\}$. The powers are set such that the reception region of s_1 is not connected (the two SINR reception islands of s_1 are represented by the two white circles with dashed boundaries). However, it is connected when restricting it to a given connected component of the weighted Voronoi region of s_1. The network $\mathcal{A}$ is then transformed into another network $\mathcal{A}'$ (shown in the bottom figure) by replacing each interfering station $s_i \in S \setminus \{s_1\}$ by sufficiently many copies of interfering stations $S_i = \{s_i^1, \ldots, s_i^m\}$ co-located at the location of s_i, each transmitting with power $\psi_i' = \psi_i/m$. Hence, by Eq. (5), all the interfering stations have a very small weight in the corresponding weighted Voronoi diagram. Since the total interference experienced by any point $p \in H(s_1, \mathcal{A})$ is the same in both networks, the reception region of s_1 is preserved (i.e., $H(s_1, \mathcal{A}) = H(s_1, \mathcal{A}')$). By taking m to be sufficiently large, the influence of s_1 is increased tremendously in the corresponding weighted Voronoi diagram for network $\mathcal{A}'$. This results in a very large connected weighted Voronoi region for s_1, which contains the two disconnected SINR reception components of s_1.

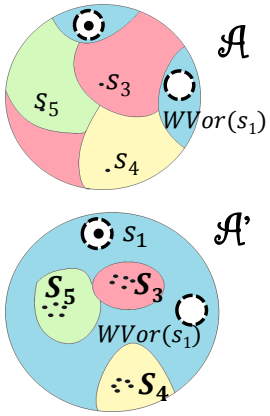

5 SINR Diagram with Interference Cancellation and High Order Voronoi Diagram

Finally, we turn to consider the third setting for studying wireless networks in which the reception points are allowed to employ a decoding technique, known as *Interference cancellation* (IC). IC is a relatively recent and promising method

for efficient decoding [1]. The basic idea of interference cancellation, and in particular *successive interference cancellation (SIC)*, is quite simple. First, the strongest interfering signal is detected and decoded. Once decoded, this signal can then be subtracted ("cancelled") from the original signal. Subsequently, the next strongest interfering signal can be detected and decoded from the now "cleaner" signal, and so on. Optimally, this process continues until all interferences are cancelled and we are left with the desired transmitted signal, which can now be decoded. It should be noted that without using IC, every station can decode at most one transmission (i.e., the strongest signal it receives). In contrast, with IC, every station can decode more transmissions, or expressed dually, every transmitter can reach more receivers. This clearly increases the utilization of the network. Interference cancellation is fairly well-studied from an information-theoretic point of view [21, 9, 23, 12].

Recently, [5] studied the reception regions of a wireless network in the SINR model with receivers that employ SIC. We next formally define the SIC-SINR diagrams, then define a generalization of Voronoi diagram known as, *high-order Voronoi diagram*, and finally describe the connection between these diagrams, established in [5].

SIC-SINR Diagrams in Uniform Power Networks. SIC changes the basic criterion for a successful reception, and hence it calls for new definitions of the reception regions that form the *SIC-SINR Diagrams*.

Let $\mathcal{A} = \langle d, S, \psi = \overline{1}, N, \beta > 1, \alpha \rangle$ be an n-station uniform power wireless network. For a subset $S' \subseteq S$, let $\mathcal{A}(S') = \langle d, S', \psi = \overline{1}, N, \beta > 1, \alpha \rangle$ be the network induced on a subset of stations S'. Let $\overrightarrow{S_i} = \{s_{i_1}, \ldots, s_{i_k}\} \subseteq S$ be an ordering of k stations.

We begin by defining the reception area $H(\overrightarrow{S_i})$ of all points that receive s_{i_k} correctly after successive cancellation of $s_{i_1}, \ldots, s_{i_{k-1}}$. For every $j \in \{2, \ldots, k\}$, let $S_{i,j} = S \setminus \{s_{i_1}, \ldots, s_{i_{j-1}}\}$ be the subset of stations excluding the first $j-1$ stations in the ordering $\overrightarrow{S_i}$ and let $S_{1,j} = S$. The reception region $H(\overrightarrow{S_i})$ is defined by

$$H(\overrightarrow{S_i}) = \bigcap_{j=1}^{k} H(s_{i_j}, \mathcal{A}(S_{i,j})) \ , \tag{6}$$

where $H(s_{i_j}, \mathcal{A}(S_{i,j}))$ is given by Eq. (2). The reception region $H^{SIC}(s_1)$ consists of all points that can receive the transmission of s_1 by employing interference cancellation. Hence, it is the union of all $H(\overrightarrow{S_i})$ regions for which that last station $\mathsf{Last}(\overrightarrow{S_i})$ is s_1.

$$H^{SIC}(s_1) = \bigcup_{\overrightarrow{S_i} \ | \ \mathsf{Last}(\overrightarrow{S_i}) = s_1} H(\overrightarrow{S_i}) \ . \tag{7}$$

The fundamental result of [5] states that although potentially there are exponentially many possible cancellation orderings $\overrightarrow{S_i}$ with $\mathsf{Last}(\overrightarrow{S_i}) = 1$, and as a result, disconnected reception components in $H^{SIC}(s_1)$, in fact there are only

$O(n^{2d})$ orderings $\overrightarrow{S_i}$, $\mathsf{Last}(\overrightarrow{S_i}) = s_1$ with nonempty reception regions $H(\overrightarrow{S_i})$. The final SIC-SINR diagram consists of n reception regions $H^{SIC}(s_1), \ldots, H^{SIC}(s_n)$ and the complementary region, the null region $H^{SIC}(\emptyset)$ in which none of the stations can be received, despite the ability to employ SIC.

SIC-SINR diagrams are related to higher order Voronoi digrams, a natural extension of the ordinary Voronoi, briefly defined next.

Higher order Voronoi diagrams. In higher order Voronoi diagrams the cells are generated by more than one generator. Such diagrams provide tessellations where each region consists of the collection of points having the same k (ordered or unordered) closest points in S, for some given integer k. The are two variants of high order Voronoi diagrams: ordered (in which the order of the generator set matters) and non-ordered. SIC-SINR diagrams are related to the former.

Ordered Order-k Voronoi diagram. Let $\overrightarrow{S_i} \subseteq S$ be an ordered set of k elements from S. When the k generators are ordered, the diagram becomes the *ordered order-k Voronoi diagram* $\mathcal{V}^{\langle k \rangle}(S)$ [19], defined as

$$\mathcal{V}^{\langle k \rangle}(S) = \{\textsc{Vor}(\overrightarrow{S_i})\},$$

where the ordered order-k Voronoi region $\textsc{Vor}(\overrightarrow{S_i})$, $|\overrightarrow{S_i}| = k$, is defined as

$$\begin{aligned}\textsc{Vor}(\overrightarrow{S_i}) = \{p \in \mathbb{R}^d \mid \operatorname{dist}(p, s_{i_1}) \leq \operatorname{dist}(p, s_{i_2}) \leq \ldots \\ \leq \operatorname{dist}(p, s_{i_k}) \leq \min(\operatorname{dist}(p, S \setminus S_i))\}.\end{aligned}$$

Note that each $\textsc{Vor}(\overrightarrow{S_i})$ is an intersection of k convex shapes and hence it is convex as well. Schematic illustration for $k = 2$ is provided in Fig. 4. For example, the region $\textsc{Vor}(s_1, s_2)$ consists of all points whose nearest neighbor is s_1 and whose second nearest neighbor is s_2. Similarly, the region $\textsc{Vor}(s_2, s_1)$ consists of all points whose nearest neighbor is s_2 and whose second nearest neighbor is s_1.

SIC-SINR diagrams and Ordered Order-k Voronoi diagrams. The relation between a nonempty reception region $H(\overrightarrow{S_i})$, $\overrightarrow{S_i} = \{s_{i_1}, \ldots, s_{i_k}\}$ and an nonempty ordered order-k polygon $\textsc{Vor}(\overrightarrow{S_i})$ is given in the next lemma.

Lemma 3 ([5]). *$H(\overrightarrow{S_i}) \subseteq \textsc{Vor}(\overrightarrow{S_i})$, for $\beta \geq 1$.*

This relation was used by [5] to provide the following characterization of SIC-SINR reception regions: every region $H^{SIC}(s_i)$ is composed of a collection of convex regions, each of which is contained in corresponding cell of the higher-order Voronoi diagram. Fig. 5 illustrates this relation, and shows the reception region $H^{SIC}(s_1)$. The light grey region $H(s_1)$ corresponds to the ordinary reception region with no cancellation. The black region $H(s_2, s_3, s_1)$ consists of

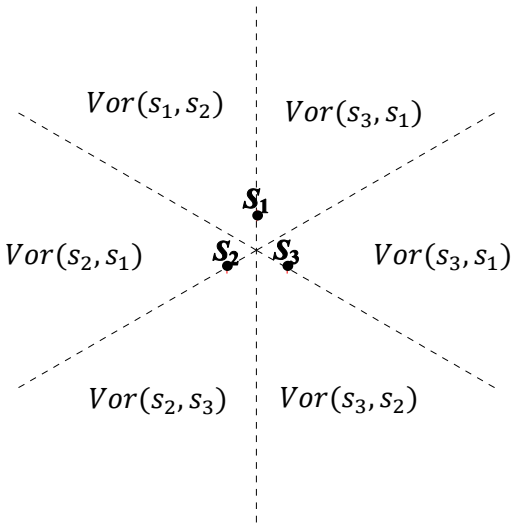

Fig. 4. A system of 3 points s_1, s_2, s_3 and their ordered order-2 Voronoi diagram.

all points that first decoded s_2, cancelled it, then decoded s_3 and cancelled it, and finally were able to decode s_1. Each of these connected reception regions is fully contained in their corresponding high order Voronoi regions. For example, the black region $H(s_2, s_3, s_1)$ is contained in the high order Voronoi region $\textsc{Vor}(s_2, s_3, s_1)$ (i.e., the set of all points whose first nearest neighbor is s_2, then s_3 and finally s_1.) Finally, SIC-SINR diagrams are also shown to be related to *hyperplane arrangements* [10], a plane-tessellation formed by the intersection of the set of $\binom{n}{2}$ hyperplane of pairs in S.

Applications. The connections to both high-order Voronoi diagram and hyperplane arrangements play a key role in [5] where it used to provide to (1) the topological characterization of SIC-SINR regions and (2) algorithms for these diagrams. Specifically, these connections are used for establishing a bound of $O(n^{2d+1})$ on the number of components in d-dimensional n-station networks. In addition, they yeild algorithmic applications for drawing and maintaining SIC-SINR diagram as well as for answering efficiently point-location queries.

6 Final Note: Towards Wireless Computational Geometry

A major long-term goal of the study of SINR diagrams is to develop the area of "wireless computational geometry" in which SINR diagrams play a role that is similar to that of Voronoi diagrams in computational geometry. Indeed, this review aimed at highlighting the intimate connections between these models

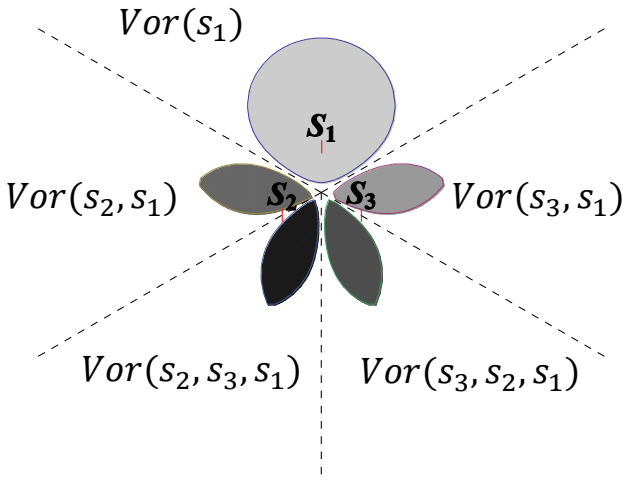

Fig. 5. The relation between the SIC-SINR diagram and the high-order Voronoi diagram.

which encourages further study of SINR diagrams in more realistic settings (e.g., adding obstacles, directional antennas, etc.) and their Voronoi counterparts.

References

1. J.G. Andrews. Interference cancellation for cellular systems: a contemporary overview. *Wireless Communications, IEEE*, 12(2):19 – 29, 2005.
2. M. Andrews and M. Dinitz. Maximizing capacity in arbitrary wireless networks in the SINR model: Complexity and game theory. In *Proc. INFOCOM*, 2009.
3. B. Aronov and M.J. Katz. Batched point location in SINR diagrams via algebraic tools. *CoRR*, abs/1412.0962, 2014.
4. F. Aurenhammer and H. Edelsbrunner. An optimal algorithm for constructing the weighted voronoi diagram in the plane. *Pattern Recognition*, 17:251–257, 1984.
5. C. Avin, A. Cohen, Y. Haddad, E. Kantor, Z. Lotker, M. Parter, and D. Peleg. SINR diagram with interference cancellation. In *Proc. SODA*, pages 502–515, 2012.
6. C. Avin, Y. Emek, E. Kantor, Z. Lotker, D. Peleg, and L. Roditty. SINR diagrams: Convexity and its applications in wireless networks. *J. ACM*, 59(4), 2012.
7. C. Avin, Z. Lotker, and Y.-A. Pignolet. On the power of uniform power: Capacity of wireless networks with bounded resources. In *Proc. ESA*, pages 373–384, 2009.

8. F. Baccelli and B. Blaszczyszyn. Stochastic geometry and wireless networks volume 1: Theory. *Foundations and Trends in Networking.*, 3:249–449, 2009.
9. M. Costa and A. El-Gamal. The capacity region of the discrete memoryless interference channel with strong interference. *IEEE Trans. Inf. Th.*, 33:710–711, 1987.
10. H. Edelsbrunner. *Algorithms in Combinatorial Geometry.* Springer-Verlag, 1987.
11. H. Edelsbrunner, D. Kirkpatrick, and R. Seidel. On the shape of a set of points in the plane. *IEEE Trans. Inf. Th.*, 29(4):551–559, 1983.
12. R.H. Etkin, D.N.C. Tse, and H. Wang. Gaussian interference channel capacity to within one bit. *IEEE Trans. Inf. Th.*, 54(12):5534–5562, 2008.
13. A. Goldsmith. *Wireless Communications.* Cambridge University Press, 2005.
14. O. Goussevskaia, R. Wattenhofer, M.M. Halldórsson, and E. Welzl. Capacity of arbitrary wireless networks. In *Proc. INFOCOM*, pages 1872–1880, 2009.
15. P. Gupta and P.R. Kumar. The capacity of wireless networks. *IEEE Trans. Inf. Th.*, 46(2):388–404, 2000.
16. M.M. Halldórsson and R. Wattenhofer. Wireless communication is in APX. In *Proc. ICALP*, pages 525–536, 2009.
17. E. Kantor, Z. Lotker, M. Parter, and D. Peleg. The topology of wireless communication. In *Proc. STOC*, 2011.
18. T. Moscibroda. The worst-case capacity of wireless sensor networks. In *Proc. IPSN*, pages 1–10, 2007.
19. A. Okabe, B. Boots, K. Sugihara, and S.N. Chiu. *Spatial Tesselations.* Princeton University Press, 1992.
20. A. Ozgur, O. Leveque, and D. Tse. Hierarchical cooperation achieves optimal capacity scaling in ad hoc networks. *IEEE Trans. Inf. Th.*, 53:3549–3572, 2007.
21. H. Sato. The capacity of the gaussian interference channel under strong interference. *IEEE Trans. Inf. Th.*, 27(6):786–788, 1981.
22. D. Tse and P. Viswanath. *Fundamentals of Wireless Communication.* Cambridge University Press, 2005.
23. A.J. Viterbi. Very low rate convolution codes for maximum theoretical performance of spread-spectrum multiple-access channels. *IEEE J. Selected Areas in Communications*, 8(4):641–649, 1990.